

CORRESPONDENCE OPEN



Genomic and immunogenomic profiling of extramedullary acute myeloid leukemia reveals actionable clonal branching and frequent immune editing

© The Author(s) 2025

Blood Cancer Journal (2025)15:136; <https://doi.org/10.1038/s41408-025-01345-2>

Dear Editor:

Acute myeloid leukemia (AML) originates in the bone marrow (BM), but in some patients, leukemic cells infiltrate peripheral tissues such as the skin (*leukemia cutis*) or other organs (*myeloid sarcoma*), a phenomenon known as extramedullary AML (eAML). eAML can present at initial diagnosis, during relapse after chemotherapy or allogeneic hematopoietic cell transplantation (allo-HCT), either in isolation or concurrently with BM involvement [1]. While symptomatic eAML is reported in approximately 2% of de novo AML cases, recent imaging-based studies suggest its true prevalence may exceed 20% [2].

Despite its clinical relevance, the prognostic significance of eAML remains unclear, with retrospective studies reporting conflicting outcomes [1]. A key limitation in interpreting these data is the common assumption that extramedullary lesions are biologically and genetically similar to BM disease. Reflecting this notion, the 2022 European Leukemia Network (ELN) guidelines offer no specific recommendations for the diagnosis or management of eAML [3]. As a result, molecular profiling of eAML is rarely performed when BM disease is also present, and routine screening at AML diagnosis is lacking—contributing to the underdiagnosis of clinically silent extramedullary disease.

Interestingly, eAML incidence is higher after allo-HCT [4, 5], often as a solitary site of relapse, raising the possibility that immune evasion contributes to its development. In the post-transplant setting, AML relapse is often driven by downregulation [6, 7] or genomic loss [8] of human leukocyte antigen (HLA), allowing leukemic cells to escape graft-versus-leukemia surveillance. This parallel raises the question of whether similar immune escape mechanisms might also underlie extramedullary dissemination outside of the transplant context. Currently, no study has systematically explored this possibility.

Furthermore, few genomic studies have analyzed paired BM and eAML specimens to determine whether leukemia cells at extramedullary sites follow distinct evolutionary trajectories. The existing studies have relied on heterogeneous, limited gene panels that excluded immune-related loci, like *HLA* and killer-cell immunoglobulin-like receptor (*KIR*) genes [9–12].

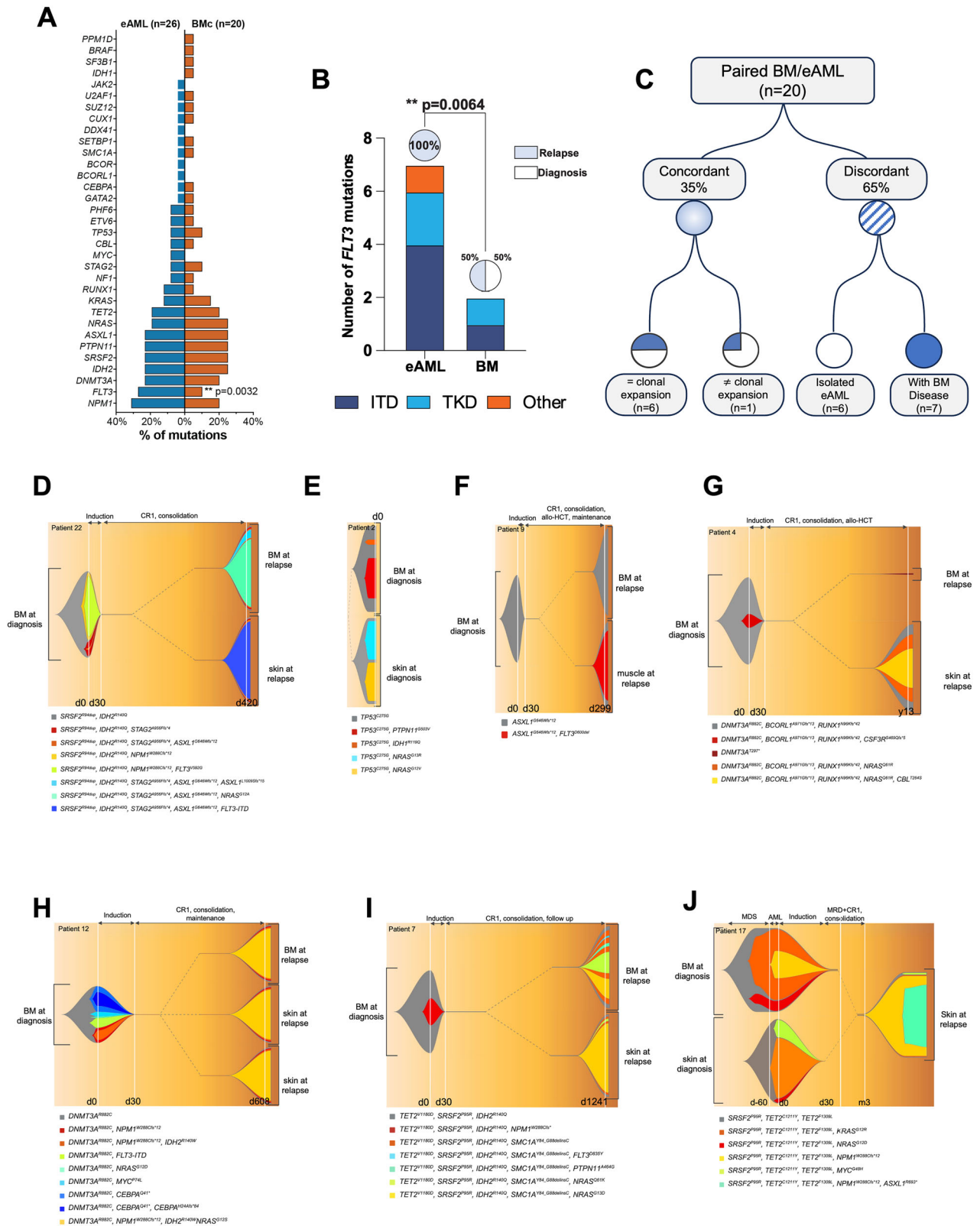
To address these limitations, we analyzed paired BM and eAML samples from 26 patients retrospectively identified from two institutions (Nancy University Hospital and Washington University in St. Louis) between 2004 and 2023 (*Study Overview*). All cases had available formalin-fixed paraffin-embedded (FFPE) extramedullary tissue and 20 also had matched cryopreserved BM DNA. Patient characteristics

(Table S1), and sample configurations are detailed in the Supplementary Materials (Fig. S1A, B and Table S2). Control cohorts included 97 healthy individuals from the 1000 Genomes Project [13] and an AML cohort from the Beat AML [14] dataset that excluded cases with documented extramedullary disease. Whole-exome sequencing (WES) was performed with an average coverage of 246x. Sequencing reads were aligned to the reference GRCh38, and variants, including single nucleotide variants (SNVs) and structural variants (SVs) such as indels, inversions, and copy number variation (CNVs), were identified using the DRAGEN pipeline and annotated with ANNOVAR (version 2020-06-08), Variant Effect Predictor (version 112, May 2024) and AnnotSV (version 3.4.1, 2024). Variants were filtered based on sequencing depth and allele frequency threshold and visually validated in Integrative Genomic Viewer. Germline variants were excluded based on public databases and matched clinical sequencing. Clonal evolution was assessed using normalized variant allele frequencies (nVAF), scaled within each sample to correct for tumor purity. *HLA* and *KIR* genotyping were performed using the NovoHLA pipeline, which enables allele-level resolution across classical and nonclassical loci and was developed and validated in our previous work [8]. Allelic loss and loss of heterozygosity (LOH) events were inferred from allelic imbalance and supported by exon-level read depth comparisons. Statistical analyses included the Wilcoxon matched pairs signed rank test at 95% CI for comparisons of continuous variables, Fisher's exact test for categorical comparisons between independent groups, and ANOVA for multiple groups comparison. Multiple testing correction was performed using the Benjamini–Hochberg procedure. Analyses were performed in GraphPad Prism and R (v4.2.0), using standard packages (Supplementary methods).

EAML LESIONS ARE ENRICHED IN *FLT3* MUTATIONS AT RELAPSE AND FREQUENTLY EXHIBIT CLONAL DIVERGENCE FROM PAIRED BONE MARROW SAMPLES

Mutational analysis of recurrently mutated genes in AML (Fig. S2A and Table S3) identified pathogenic variants in 92% of samples, including BM specimens with no morphologic blasts. *FLT3* and *NPM1* were the most common eAML mutations (27% and 31%, respectively), whereas paired BM samples more frequently harbored *IDH2*, *SRSF2*, *PTPN11*, *ASXL1*, and *NRAS* (Fig. 1A). *FLT3* mutations were significantly enriched in eAML versus paired BM (25% vs. 10%, Fisher's exact $p = 0.0032$), with an odds ratio of 3.3. Importantly, five *FLT3* mutations (including *ITD*, *TKD*, and *D600del*) were detected exclusively in eAML, absent from paired BM and diagnostic BM samples. In contrast, five cases showed *FLT3* mutations at diagnosis that were subsequently lost in both eAML and BM at relapse (Table S4 and Fig. S2B). All eAML *FLT3* mutations were observed in eAML lesions detected at relapse, whereas only

Received: 4 May 2025 Revised: 8 July 2025 Accepted: 30 July 2025
Published online: 13 August 2025



one was present in a relapsed BM (Fisher's exact $p = 0.0064$, Fig. 1B). The overall SV burden was comparable between BM and eAML (Fig. S3A, B). eAML exhibited a higher frequency of small (<150 bp) inversions, while large deletions (>500 kb) were more

common in BM samples (Fig. S3C). Genes recurrently impacted by SVs in eAML included *CSF3R*, *NPM1*, *NRAS*, and *PTPN11* (Fig. S3D). Clonal evolution analysis, using nVAF and visualized via fishplots [15], showed discordant mutational profiles in 65% of paired BM/

Fig. 1 Clonal divergence and distinct mutational profiles of extramedullary AML compared to paired bone marrow disease.

A Comparative mutation frequency analysis of eAML and concurrent bone marrow samples. Bar plot illustrating the frequency of gene mutations in extramedullary AML samples (eAML, blue) compared to paired, concomitant bone marrow samples (BMc, orange), *FLT3* mutations are enriched in eAML cases compared to paired BM samples (Fisher's exact $p = 0.0032$). **B** *FLT3* mutation frequency and distribution between eAML and bone marrow samples. Stacked bar chart comparing the number and types of *FLT3* mutations between eAML and BM (all samples). *FLT3* mutations, including internal tandem duplications (ITD) and tyrosine kinase domain (TKD) mutations, were more prevalent at relapse and significantly enriched in eAML sites compared to BM samples (Fisher's exact $p = 0.0064$). **C** Site-specific clonal evolutionary trajectories. Categorization of the 20 paired eAML and BM samples, showing: concordant mutational status ($n = 7$): cases in which BM and eAML shared highly similar mutational profiles, suggesting a common clonal origin with minimal divergence. Nearly all exhibited equivalent variant allele frequencies (nVAFs) for key mutations in both compartments, indicating parallel evolution of dominant clones (Patient IDs: 6, 12, 15, 19, 28, 29). One case (Patient ID: 7) showed differences in nVAFs between BM and eAML. Discordant mutational status ($n = 14$): cases in which BM and eAML displayed distinct mutational landscapes, suggesting independent clonal evolution. These are further classified as: • Concomitant BM involvement ($n = 7$; Patient IDs: 2, 9, 10, 13, 17, 21, 22): leukemia was detected in both BM and extramedullary sites. • Isolated eAML ($n = 6$; Patient IDs: 1, 4, 8, 18, 24, 27): the paired BM lacked morphologic evidence of leukemia but harbored genetic alterations. **D–J** Fish plots illustrating distinct patterns of clonal evolution in eAML versus BM sites. Mutations are color-coded according to the legend. **D–F** show cases of concomitant BM and eAML with discordant mutational profiles. These cases indicate divergent evolutionary trajectories and potential site-specific selective pressures driving leukemic progression. **G** illustrates an isolated myeloid sarcoma relapse with no detectable BM involvement at relapse, demonstrating spatially restricted clonal evolution. **H–I** Represent cases of concordant mutational profiles in BM and eAML, with similar clonal expansion patterns (**H**), or different clonal expansion (**I**). **J** presents progressive eAML lesions containing subclones derived from both BM and the initial eAML site at diagnosis, highlighting intercompartmental clonal exchange.

eAML samples (Fig. 1C). These included eAML-specific subclones absent from BM (Fig. 1D, E), or ancestral clones acquiring cooperating mutations exclusively in eAML, as observed in post-transplant relapses, where BM often harbored clonal hematopoiesis-associated mutations, while eAML lesions showed clear leukemic evolution (Fig. 1F, G). In 35% of cases, BM and eAML shared concordant profiles (Fig. 1H), though some showed differential clonal expansion (Fig. 1I). Notably, progressive eAML lesions sometimes derived from both BM and initial eAML clones (Fig. 1J), emphasizing the complexity of clonal dynamics. Across these cases, actionable mutations in *FLT3*, *IDH2* genes, and potentially actionable mutations in *RAS* genes were frequently observed in eAML but not in BM. Despite this divergence, mutational signature analysis using SigProfiler [16] revealed that both BM and eAML samples were dominated by SBS1 and SBS5 (endogenous aging processes), and no organ-specific mutational signature was identified (Fig. S4).

RAS PATHWAY MUTATIONS AND HLA ALTERATIONS AS BIOMARKERS OF EAML RISK

To identify features associated with risk of eAML development, we compared BM samples from our eAML cohort to 483 de novo AML cases in the BeatAML dataset (excluding cases with documented eAML). *RAS/MYC* pathway mutations (*PTPN11*, *NRAS*, *KRAS*, *MYC*) were significantly enriched in the eAML cohort ($p = 0.0017$, Fig. 2A), with the strongest associations for *PTPN11* ($p = 0.0045$) and *MYC* ($p = 0.024$, Fig. 2B). *RAS* mutations were also enriched in BM samples paired to eAML manifestation (Fig. S5A, B). We also observed a corresponding enrichment of M5 (monocytic) AML ($p = 0.018$) and a depletion of M1 cases (AML without maturation) ($p = 0.038$, Fig. S5C), consistent with the established association between *RAS* pathway mutations and monocytic differentiation [17].

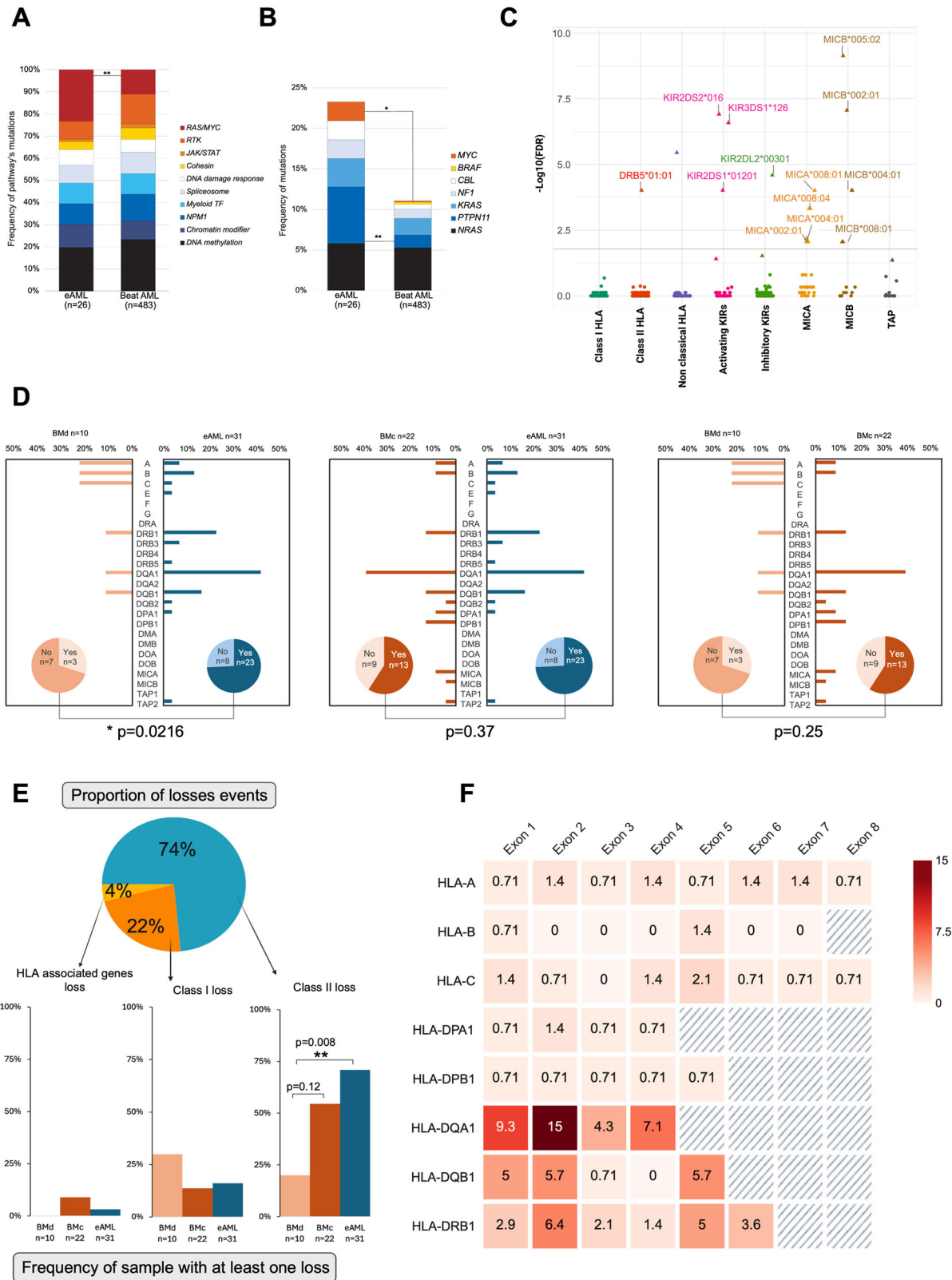
We next investigated whether immunogenetic factors may predispose to eAML dissemination, by comparing *HLA* and *KIR* genotypes with an independent healthy control cohort (supplementary methods). While no significant associations were observed between classical *HLA* alleles and eAML incidence (Fig. S6A, B), specific activating and inhibitory *KIR* alleles, as well as *MICA* and *MICB* variants, were significantly over-represented in eAML patients compared to controls. (Fig. 2C and Tables S5, S6).

We further investigated the potential role of immunogenetic escape mechanisms underlying eAML pathogenesis. Indeed, somatic alterations in *HLA class I* and *II* genes were frequent in

eAML samples. Of 78 total events, 63 were deletions and 15 LOH (Fig. S6C). *HLA* losses were significantly more common in eAML compared to BM collected at initial diagnosis, before eAML development, from the same patients (Fisher's exact $p = 0.0216$, Fig. 2D). The strongest enrichment was observed in eAML samples obtained at leukemia diagnosis or at relapse allo-HCT (Fig. S7A). *HLA* alterations were no longer enriched when eAML was compared to concurrent BM samples, suggesting that *HLA* loss likely originates in the BM and it is retained during dissemination. Class II losses predominated over class I (74% vs. 22%, $p < 0.0001$) and were significantly more common in eAML vs. BM samples without extramedullary involvement (70% vs. 20%, $p = 0.008$, Fig. 2E).

Exon-level analysis demonstrated that most *HLA class II* deletions occurred in *exon 2*, encoding the antigen-binding region, and also impacted CD4/CD8 coreceptor contact sites and leader sequences essential for protein expression (Fig. 2F). Notably, eAML cases with *NPM1*- or *FLT3*-mutations, which are often associated with *HLA class II* downregulation, tended to retain intact *HLA* loci, suggesting that mutation-driven *HLA* down-regulation mechanisms may substitute for genetic loss (Fig. S7B). When integrating all genetic immune escape events (i.e., deletions/LOH and mutations associated with *HLA class II* down-regulation), *HLA* deregulation was observed in 89% of cases (Fig. S7C), implicating immune escape as a central feature of extramedullary dissemination.

This study demonstrates that eAML frequently exhibit clonal divergence from concomitant BM disease, indicating distinct selective pressures at extramedullary sites. In some cases, eAML may evolve independently from pre-leukemic clones, as seen in a post-transplant relapse restricted to extramedullary sites with no driver mutations in the BM. We commonly observed actionable and potentially actionable mutations in eAML, including *FLT3*, *NPM1*, and *IDH2*, even when eAML was detected at diagnosis and before any treatment, underscoring the need for lesion-specific sequencing. Mutations in the *RAS* pathway were significantly more frequent in both the BM and eAML lesions of patients with extramedullary disease, consistent with their known role in promoting monocytic differentiation and tissue infiltration. Similarly, widespread *HLA class II* losses, (particularly involving *exon 2*, and additional alterations affecting CD4/CD8 T cell contact sites) were observed in both the BM and extramedullary compartments. These findings support a model in which immune escape originates in the BM and is retained or selected for during dissemination to extramedullary sites. Together, these data suggest that *RAS*



mutations and *HLA* alterations may serve as predictive biomarkers of eAML risk and guide early surveillance and therapeutic decision-making.

Based on our findings we advocate for active screening for extramedullary involvement at AML diagnosis, as eAML frequently

harbors actionable mutations that may be missed without lesion-specific profiling. Incorporating eAML into MRD monitoring frameworks is also warranted, particularly given its association with immune escape mechanisms and relapse. Finally, systematic assessment of *RAS* pathway mutations and *HLA* losses in the BM

Fig. 2 RAS pathway mutations and HLA alterations as biomarkers of eAML Risk. **A** Stacked bar plot illustrating the frequency of mutations across key functional categories in BM samples from eAML ($n=26$) and BeatAML ($n=483$). Categories include DNA methylation, chromatin modifiers, *NPM1*, myeloid transcription factors (TFs), spliceosome components, DNA damage response, cohesin, *JAK/STAT* signaling, receptor tyrosine kinases (RTKs), and the *RAS/MYC* pathway. Mutations in the *RAS/MYC* pathway are significantly enriched in the BM of cases with eAML ($**p=0.0017$). **B** Stacked bar plot comparing the prevalence of mutations in *RAS* pathway genes (*NRAS*, *PTPN11*, *KRAS*, *NF1*, *CBL*, *BRAF*, and *MYC*) between bone marrow samples from eAML ($n=26$) and BeatAML ($n=483$). Significant differences are indicated: $*p=0.024$; $**p=0.0045$. **C** Enrichment analysis of immune alleles in eAML versus healthy controls. The $-\log_{10}(\text{FDR})$ values for various alleles are shown, highlighting statistically significant overrepresentation in eAML, particularly within activating *KIR* alleles (*KIR2DS2*, *KIR2DS1*, *KIR2DS5*), inhibitory *KIR* alleles (*KIR2DL3*), and *MICA/MICB* alleles. Points above the dashed lines are significant. **D** Comparison of HLA losses between BM and eAML samples. Bar plots display the frequency of HLA losses in class I and class II genes across patient subgroups. Pie charts below each plot indicate the proportion of samples harboring at least one HLA loss. **E** Proportion of HLA loss events across class I, class II, and non-classical HLA genes. The pie chart illustrates the relative distribution of HLA losses among class I, class II, and nonclassical HLA genes. Below, bar plots show the frequency of samples with at least one loss, stratified by disease compartment and HLA gene class. **F** HLA loss distribution across exons. Heatmap showing the frequency of deletions and LOH events across exons of different HLA genes. Exon 2 of HLA class II genes exhibited the highest density of genetic losses.

may help identify patients at increased risk of developing extramedullary disease and should guide future risk-adapted treatment strategies.

Clément Collignon^{1,2}, Tucker Hansen³, Colin Hercus⁴, Marianna B. Ruzinova⁵, Gabrielle Roth Guepin², Caroline Bonmati², Marie Thérèse Rubio^{2,6}, Pierre Feugier², Mélanie Gaudfrin⁶, Hervé Sartelet⁷, Marion Divoux⁸, Marc Muller⁸, Sharon Heath¹, Geoffrey L. Uy¹, David H. Spencer¹, David Y. Chen³, Simona Pagliuca^{2,6} and Francesca Ferraro¹✉
¹Division of Oncology – Hematologic Malignancies, Transplant and Cellular Therapy, Washington University in Saint Louis, Saint Louis, MO, USA. ²Hematology Department, Nancy University Hospital, Vandoeuvre-lès-Nancy, France. ³Division of Dermatology, Washington University in Saint Louis, Saint Louis, MO, USA. ⁴Novocraft Technologies Sdn Bhd, Kuala Lumpur, Malaysia. ⁵Department of Pathology and Immunology, Washington University in Saint Louis, Saint Louis, MO, USA. ⁶UMR 7365, IMoPA, University of Lorraine, Vandoeuvre-lès-Nancy, France. ⁷Department of Pathology, Nancy University Hospital, Vandoeuvre-lès-Nancy, France. ⁸Genetic Department, Nancy University Hospital, Vandoeuvre-lès-Nancy, France. ✉email: S.PAGLIUCA@chru-nancy.fr; ferrarof@wustl.edu

DATA AVAILABILITY

The sequencing files generated in this study have been deposited at the following repository <https://doi.org/10.6084/m9.figshare.28661279>. For any additional requests, please contact the corresponding authors.

REFERENCES

- Shallis RM, Gale RP, Lazarus HM, Roberts KB, Xu ML, Seropian SE, et al. Myeloid sarcoma, chloroma, or extramedullary acute myeloid leukemia tumor: a tale of misnomers, controversy and the unresolved. *Blood Rev.* 2021;47:100773.
- Stolzel F, Luer T, Lock S, Parmentier S, Kuithan F, Kramer M, et al. The prevalence of extramedullary acute myeloid leukemia detected by (18)FDG-PET/CT: final results from the prospective PETAML trial. *Haematologica.* 2020;105:1552–8.
- Dohner H, Wei AH, Appelbaum FR, Craddock C, DiNardo CD, Dombret H, et al. Diagnosis and management of AML in adults: 2022 recommendations from an international expert panel on behalf of the ELN. *Blood.* 2022;140:1345–77.
- Lee KH, Lee JH, Choi SJ, Lee JH, Kim S, Seol M, et al. Bone marrow vs extramedullary relapse of acute leukemia after allogeneic hematopoietic cell transplantation: risk factors and clinical course. *Bone Marrow Transpl.* 2003;32:835–42.
- Yoshihara S, Ando T, Ogawa H. Extramedullary relapse of acute myeloid leukemia after allogeneic hematopoietic stem cell transplantation: an easily overlooked but significant pattern of relapse. *Biol Blood Marrow Transpl.* 2012;18:1800–7.
- Christopher MJ, Petti AA, Rettig MP, Miller CA, Chendamalai E, Duncavage EJ, et al. Immune escape of relapsed AML cells after allogeneic transplantation. *N Engl J Med.* 2018;379:2330–41.
- Toffalori C, Zito L, Gambacorta V, Riba M, Oliveira G, Bucci G, et al. Immune signature drives leukemia escape and relapse after hematopoietic cell transplantation. *Nat Med.* 2019;25:603–11.

- Pagliuca S, Gurnari C, Hercus C, Hergalant S, Hong S, Dhuyser A, et al. Leukemia relapse via genetic immune escape after allogeneic hematopoietic cell transplantation. *Nat Commun.* 2023;14:3153.
- Engel NW, Reinert J, Borchert NM, Panagiota V, Gabdouline R, Thol F, et al. Newly diagnosed isolated myeloid sarcoma-paired NGS panel analysis of extramedullary tumor and bone marrow. *Ann Hematol.* 2021;100:499–503.
- Greenland NY, Van Ziffle JA, Liu YC, Qi Z, Prakash S, Wang L. Genomic analysis in myeloid sarcoma and comparison with paired acute myeloid leukemia. *Hum Pathol.* 2021;108:76–83.
- Pastoret C, Houot R, Llamas-Gutierrez F, Boulland ML, Marchand T, Tas P, et al. Detection of clonal heterogeneity and targetable mutations in myeloid sarcoma by high-throughput sequencing. *Leuk Lymphoma.* 2017;58:1008–12.
- Untaaveesup S, Trithiphen S, Kulchutisin K, Rungjirajitranon T, Leelakanok N, Panyoy S, et al. Genetic alterations in myeloid sarcoma among acute myeloid leukemia patients: insights from 37 cohort studies and a meta-analysis. *Front Oncol.* 2024;14:1325431.
- Genomes Project C, Auton A, Brooks LD, Durbin RM, Garrison EP, Kang HM, et al. A global reference for human genetic variation. *Nature.* 2015;526:68–74.
- Tyner JW, Tognon CE, Bottomly D, Wilmot B, Kurtz SE, Savage SL, et al. Functional genomic landscape of acute myeloid leukaemia. *Nature.* 2018;562:526–31.
- Miller CA, McMichael J, Dang HX, Maher CA, Ding L, Ley TJ, et al. Visualizing tumor evolution with the fishplot package for R. *BMC Genom.* 2016;17:880.
- Islam SMA, Diaz-Gay M, Wu Y, Barnes M, Vangara R, Bergstrom EN, et al. Uncovering novel mutational signatures by de novo extraction with SigProfilerExtractor. *Cell Genom.* 2022;2:None.
- Sango J, Carcamo S, Sirenko M, Maiti A, Mansour H, Ulukaya G, et al. RAS-mutant leukaemia stem cells drive clinical resistance to venetoclax. *Nature.* 2024;636:241–50.

ACKNOWLEDGEMENTS

This work was supported by a Leukemia Research Foundation grant to FF. We are grateful to the McDonnell Genome Institute at Washington University School of Medicine for their sequencing and genomic expertise. The Center is partially supported by NCI Cancer Center Support Grant #P30 CA91842. SP received funding from Fondation ARC pour la Recherche sur le Cancer, MDS Foundation Tito Bastianello Award, Force Hemato. Sample collection for Washington University is supported by the Specialized Program of Research Excellence in Acute Myeloid Leukemia grant (P50 CA171963). We thank the Siteman Cancer Center's scientific editor, Megan Noonan, PhD, for her insightful suggestions, which enhanced the clarity and quality of this work. We thank Agata Gruszczynska for help with the initial fastq files processing. We thank all the patients and families who participated in this study.

AUTHOR CONTRIBUTIONS

CC, SP, and FF designed the study, collected, analyzed, and interpreted the data, performed the bioinformatic and statistical analyses, and wrote the manuscript. SP and CH performed immune gene analysis and visualization. CH developed NovoHLA and the methodology for the calculation of copy number variation. GRG, MTR, CB, PF, MR, SH, and GU participated in patient recruitment and management. MG, HS, MM, and MD participated in sample recruitment. DS helped in data collection and interpretation and supervised genomic experiments. DC and TH participated in study conception, sample and data collection, data interpretation, gave important intellectual inputs, and edited the manuscript. All authors participated in the analysis, interpretation, and critical manuscript revision.

COMPETING INTERESTS

The authors declare no competing interests.

ETHICS APPROVAL AND CONSENT TO PARTICIPATE

All methods were performed in accordance with the relevant guidelines and regulations. Informed consent was obtained from all participants for the use of residual biological specimens collected during clinical sampling for sequencing purposes. Ethics approval was obtained from the following institutional review boards: Nancy University Hospital Ethics Committee (IRB Nancy n° 2024PI205-290) and the Washington University in St. Louis Institutional Review Board (IRB #201011766). This study does not include any identifiable images or other personal details of participants.

ADDITIONAL INFORMATION

Supplementary information The online version contains supplementary material available at <https://doi.org/10.1038/s41408-025-01345-2>.

Correspondence and requests for materials should be addressed to Simona Pagliuca or Francesca Ferraro.

Reprints and permission information is available at <http://www.nature.com/reprints>

Publisher's note Springer Nature remains neutral with regard to jurisdictional claims in published maps and institutional affiliations.



Open Access This article is licensed under a Creative Commons Attribution-NonCommercial-NoDerivatives 4.0 International License, which permits any non-commercial use, sharing, distribution and reproduction in any medium or format, as long as you give appropriate credit to the original author(s) and the source, provide a link to the Creative Commons licence, and indicate if you modified the licensed material. You do not have permission under this licence to share adapted material derived from this article or parts of it. The images or other third party material in this article are included in the article's Creative Commons licence, unless indicated otherwise in a credit line to the material. If material is not included in the article's Creative Commons licence and your intended use is not permitted by statutory regulation or exceeds the permitted use, you will need to obtain permission directly from the copyright holder. To view a copy of this licence, visit <http://creativecommons.org/licenses/by-nc-nd/4.0/>.

© The Author(s) 2025